MEMS/NEMS development for Space Applications at NASA/JPL

Thomas George
Supervisor, MEMS Technology Group
In Situ Technology and Experiments Systems Section, Jet Propulsion Laboratory,
California Institute of Technology, Pasadena, CA 91109
Web: http://mems.jpl.nasa.gov

ABSTRACT

This paper presents an overview of the current technology development activities of the MEMS Technology Group at JPL. The group, in collaboration with other research groups at JPL and outside institutions, pursues the development of a wide range of MEMS/NEMS technologies that are primarily applicable to NASA's needs in the area of robotic planetary exploration. The broad classes of technologies being developed include inertial guidance devices, micro-propulsion devices, adaptive optics for telescope applications, micro-instruments and nano-mechanical resonator devices. End-to-end prototype development of these MEMS/NEMS technologies is conducted at JPL's state-of-the-art Microdevices Laboratory. The group is also pursuing the establishment of a rapid, space-testing program in collaboration with the Aerospace Corporation, in an effort to overcome the traditional barriers to the insertion of new technologies into space missions.

Keywords: MEMS, NEMS, space, NASA, JPL, inertial guidance, micro-propulsion, micro-instruments, TRL, PICOSAT,

INTRODUCTION

Size, mass and power consumption for devices and instruments are severely constrained on space missions. Therefore, Micro/Nano Electro Mechanical Systems (MEMS/NEMS) technologies are uniquely suited for space applications since they offer the advantages of low mass, low power consumption and reliability, with novel capabilities. Given the prohibitive costs of launching any payload into space (between $10,000 - $1000,000 per kg, depending on the type of mission), the trend during the past decade has been towards "smaller, faster and cheaper" space missions. Such missions are necessarily of the "micro-spacecraft" class (under 100 kg mass). Several micro-spacecraft missions have been proposed or are currently under development by NASA[1]. Thus MEMS/NEMS technology is expected not only to enable future micro-spacecraft missions but also to benefit conventional missions by allowing a high degree of redundancy through deep reductions in the masses of several spacecraft and payload systems.

However, just as with the insertion of new technologies into the commercial sector, the development of new technologies for space applications faces significant challenges in ultimately being inserted into space missions. NASA has developed a now widely accepted "Technology Readiness Level" (TRL) scale to evaluate the maturity of devices being developed for space applications (Fig. 1). The TRL scale ranges from TRL1 (Basic Technology Research) to TRL 9 (Space Proven Technology). Most of the technologies being developed by the JPL MEMS Technology Group are in the range of TRL1 – TRL3. The group pursues these technology developments in collaboration with

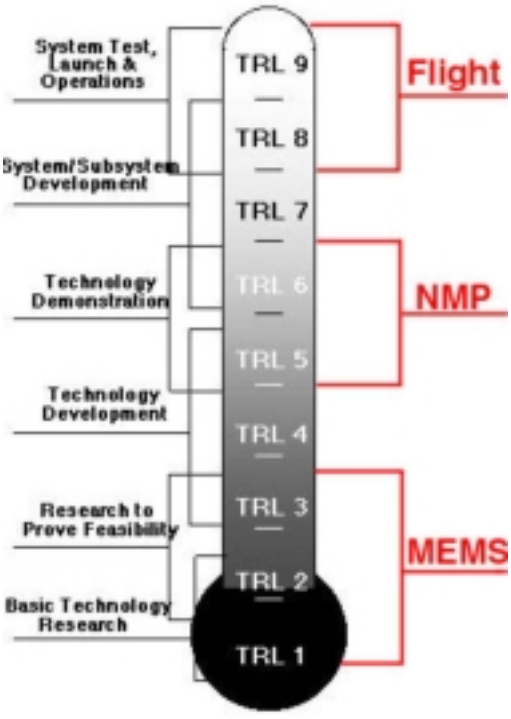

Figure 1: The NASA "Technology Readiness Level" (TRL) scale, which is used to assess the maturity of space-relevant technologies.

other groups at JPL and several outside institutions. The development path to the ultimate, successful insertion of MEMS technologies into space missions is a long and arduous one. Demonstration of "proof-of-concept" is in most cases insufficient for convincing mission planners to adopt the technology. Rather, demonstrated reliable operation in a relevant (space) environment of sub-systems or systems is required before a particular technology can compete for selection. On rare occasions the insertion of a particular technology can be accelerated, if it can be shown that the technology is revolutionary enough to enable a new mission or a new class of missions. An example of such a revolutionary MEMS technology is the "Spider Web Bolometer"[2] (described below). Recognizing the tremendous barrier that exists both in time and expense for the successful insertion of new technologies into space missions, NASA instituted a "New Millenium Program[2]" (represented by NMP in Fig. 1) with the specific charter of conducting space demonstrations of new technologies. NMP typically selects technologies at TRL 4 – 6 for space demonstration flights. However, the NMP has limited flight opportunities. Therefore, the MEMS Technology Group, in collaboration with the Aerospace Corporation, is pursuing the establishment of a "PICOSAT"-based space testing program for the rapid (~ 6 month launch centers), low cost (~ $100, 000/ mission) testing of MEMS/NEMS devices in low earth orbit.

MEMS FACILITIES AT JPL

Microdevices Laboratory Facilities

The Microdevices Laboratory is a 38,000 square foot facility with around 5,500 ft^2 each of clean room processing and device characterization laboratory space. The clean rooms are partitioned into four categories: class 10, class 100, class 1000 and class 100,000. The MDL is equipped to provide end-to-end fabrication, characterization and rapid prototyping of silicon, compound semiconductor and superconductor devices. MDL facilities include the following:

- ***Lithography***: High resolution (<0.01 μm) electron-beam lithography, 5X stepper, and double-sided contact aligners.
- ***Material deposition***: Molecular Beam Epitaxy (MBE) with in-situ characterization, Organo-Metallic Vapor-Phase Epitaxy (OMVPE), Magnetron and Diode sputtering, E-beam and Resistive Evaporation, Electron Cyclotron Resonance (ECR) Deposition, Low-Pressure Chemical Vapor Deposition (LPCVD), Plasma Enhanced Chemical Vapor Deposition (PECVD), oxidation and diffusion.
- ***Electroplating***: A state-of-the-art facility for the electro-deposition of a wide range of elements, alloys and compounds on wafer substrates is currently being set up and is in partial operation.
- ***Feature patterning:*** Acidic and alkaline wet etching, plasma and reactive ion etching, ion milling, and Deep Reactive Ion Etching (DRIE).
- ***Post-process packaging:*** Wire bonding, die separation, die attach, flip-chip aligner/bonder, and fusion/anodic/eutectic/ thermo-compression bonding.
- ***Surface and interface characterization:*** Scanning Tunneling Microscopy, Ballistic Electron Emission Microscopy, Transmission Electron Microscopy, Scanning Electron Microscopy, Atomic Force Microscopy, Electron Spectroscopy for Chemical Analysis, and X-ray diffraction.
- ***Thin-film characterization:*** Ellipsometry, stylus profilometry, optical microscopy, and interferometry.
- ***Bulk electrical and optical characterization:*** Photoluminescence (Vis, IR), four-point resistivity probe, spectrophotometry, I-V/C-V measurement, Hall measurement, and Fourier Transform Infrared Spectroscopy (FTIR).

MEMS Reliability Testing Laboratory Facilities

Reliability assurance is an integral part of the space qualification process. Over the last few decades, JPL has built a very impressive infrastructure for the reliability testing of spacecraft and instrument payloads. These facilities are being adapted for the testing of MEMS/NEMS devices and instruments being developed for space applications. Reliability testing of MEMS/NEMS devices is currently in its infancy and is complicated by the fact that there are relatively few devices available for the generation of a statistically significant database. The testing protocols are also very device dependent. The major capabilities of the Reliability Testing Laboratory include equipment for vibration and shock testing, thermal cycling, electrical stress testing, surface morphology, chemical profiling, cross-section imaging of unreleased structures, and life testing. In addition, the lab is now being expanded to include RF MEMS device testing. Subsequent to the testing, failure analysis is performed on the non-functioning devices by combining decades of experience in microelectronics failure analysis with JPL's resident expertise in a wide variety of fields, including MEMS technology, surface physics, electrical engineering, and device physics.

MEMS/NEMS TECHNOLOGY DEVELOPMENT ACTIVITIES

A representative fraction of the key research activities of the JPL MEMS Technology Group is described in brief below. MEMS/NEMS technologies are useful for a broad range of space applications, as reflected by the range of technology developments being pursued by the group in collaboration with other groups at JPL and outside institutions. Finally, the PICOSAT project for the rapid testing of MEMS/NEMS devices in space is described.

"Spider Web" Bolometer Flight Project

The Spider Web Bolometer device[3] is an excellent example of a low TRL MEMS device that has successfully made the transition to flight insertion. The Superconducting Materials & Devices Group first developed this Caltech/JPL invented device. It is hoped that the experimental measurements made by this highly sensitive device will help answer profound, fundamental questions such as the "flatness" of the expanding Universe. The 2.728 K cosmic microwave background contains anisotropies of order 10^{-5} K. Cosmological models make specific predictions about the angular and temperature scale of the anisotropies and how they vary with such parameters as the matter/energy ratio of the universe. The spider web bolometer detector is the core technology for the ESA/NASA Planck mission and the SPIRE instrument on the Herschel Space Observatory, both of which will be launched in 2007 and are expected to enable significantly higher resolution temperature and angular measurements (10^{-6}K and ~0.1-0.2 degrees) than were made heretofore by previous space missions. The device has already been used successfully on balloon missions with spectacular results[4]. The sensitivity at 100 mK (10^{-18}W/Hz$^{0.5}$) is sufficient to achieve background-limited moderate-resolution spectroscopy (R ~ 1000) from the ground. As a consequence, spider web bolometers have been "baselined" for at least 10 sub-orbital astrophysics experiments.

Figure 2. A MEMS-fabricated, SiN micromesh, "spider web" microwave detector is shown. The metallized SiN micromesh design allows for the large absorption area required for millimeter waves, coupled with extremely low heat capacity, thermal conductivity and cosmic ray cross-section. A Ge thermistor, suspended on the SiN micromesh measures the rise in temperature due to microwave absorption with a sensitivity of 10^{-18}W/Hz$^{0.5}$ at an operating temperature of 100mK.

The spider web bolometer device consists of a high-purity, neutron transmutation doped (NTD), single crystal Ge thermistor chip mounted at the center of a "spider web" consisting of metallized, suspended SiN filaments. The SiN spider web is constructed by the bulk micromachining of a silicon wafer coated with SiN grown by Low Pressure Chemical Vapor Deposition (LPCVD). The spider web structure provides a large area for microwave absorption with low heat capacity, excellent thermal isolation and a low cross-section for cosmic rays (Fig. 2). These high-sensitivity millimeter-wave bolometers typically operate at 0.1 - 0.3 K providing broadband photometry for the abovementioned astrophysics missions. The absorbed microwave radiation produces a temperature increase, which is measured by the NTD chip. The chip is attached to the spider web absorber by means of In bumps and is readout via lithographed leads. NTD Ge thermistors offer high reproducibility and excellent noise characteristics with a negligible noise background at frequencies as low as 0.01 Hz. The primary benefit for space missions from the low-frequency noise stability, is that observations can be conducted in a slow-scanned or a rastered, mode rather than requiring rapid chopping of the incoming signal in an effort to improve the detectivity. The instrument consists of feedhorn-coupled spider web bolometer devices. Feedhorn coupling provides maximum sensitivity per detector, minimizes the number of detectors, minimizes the area of each detector, and also provides control of the detector field of view.

Inertial Guidance: Miniature Vibratory Gyroscopes

Next to the Spider Web Bolometer, the Miniature Vibratory Gyroscope[5-7] devices have the highest level of maturity (TRL 4) in the group's technology portfolio. The gyroscope devices are based on a "cloverleaf" resonator design (Fig. 3), and are being developed in two flavors, an older, Silicon-on-Insulator (SOI) based Micro Gyroscope and a newer, through-wafer Meso Gyroscope (Fig. 4). The Micro Gyroscope is being targeted for non-inertial grade (1 – 10 degrees/hr bias stability) applications, whereas the Meso Gyroscope is being developed for inertial grade (0.1 – 0.01 degree/hr bias stability) applications. As shown in Table 1, the Micro Gyroscope performance is within the targeted application range, while the Meso Gyroscope being a much more recent development, has made excellent progress towards its ultimate performance goals.

The cloverleaf structure is suspended on a pair of orthogonal "springs" which are the Si beams in Fig. 3. The device is operated by initially "rocking" an adjacent pair of "petals" about one of the Si beams at its torsional resonance frequency. This is achieved by applying an ac voltage on the "drive" capacitors.

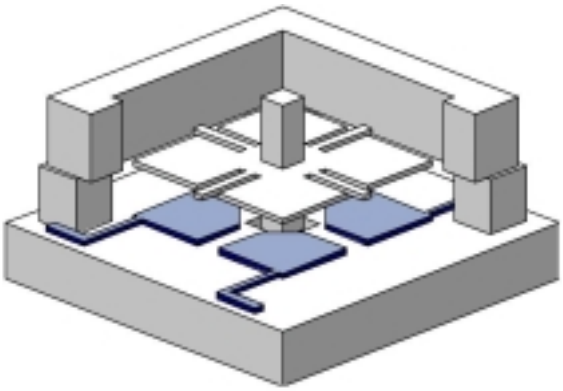

Figure 3. The structure of a single-axis, MEMS Vibratory Gyroscope device, shows the symmetric "cloverleaf" capacitor design. The central post is the inertial element, about whose axis the rotation is sensed. The "petals" of the cloverleaf are suspended on two orthogonal Si beams that form the torsional spring elements. The device operates by rocking the petals about one beam and capacitively sensing the Coriolis force-coupled motion about the orthogonal beam.

Table 1: Best Performance to-date of Miniature Gyroscopes

Parameter	*Micro Gyroscope*	*Meso Gyroscope*
Angular Bias Stability	1 degree/hour	2 degrees/hour
Angle Random Walk	0.02 degree/rt-hr	0.03 degree/rt-hr

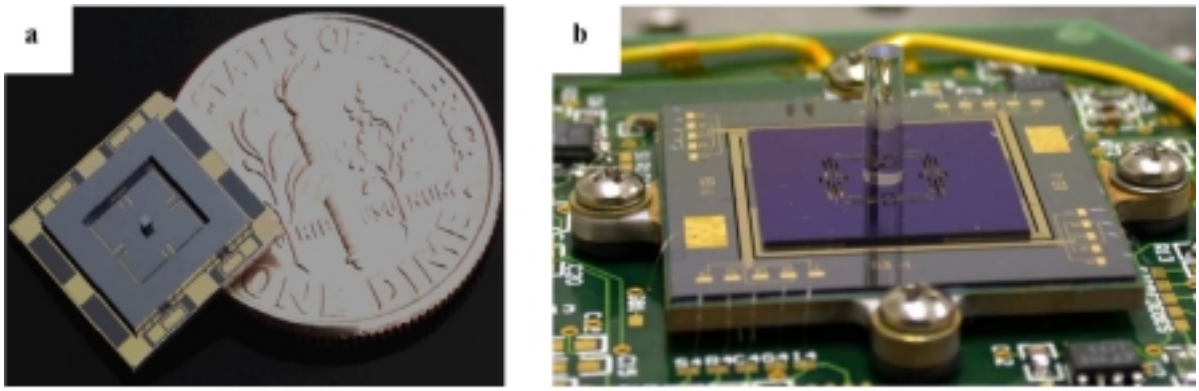

Figure 4. The two types of single-axis, miniature vibratory gyroscope devices are shown. **a)** An unpackaged, SOI-based, Micro Gyroscope device is shown. The cloverleaf design and the rotation-sensing post are clearly visible, as is the "baseplate" containing the patterned metallization for the drive and sense capacitive electrodes. **b)** A through-wafer, Meso Gyroscope device is shown mounted on a printed circuit board containing the drive circuitry. The pyrex post is anodically bonded to the cloverleaf structure.

The Coriolis force generated by the rotation-sensing post, couples the drive motion into a torsional oscillation about the orthogonal Si beam. This coupled oscillation is once again sensed capacitively. High "Q" values are of course necessary for both the drive and sense modes in order achieve low drive voltage and high sense voltage signals respectively. However, in order to achieve efficient closed loop operation of the device, with low angular bias stability, it is also critically important that the resonance frequencies of both modes be precisely matched. The Meso Gyroscope development is aimed at obtaining superior performance via a better (theoretically predicted) frequency match through the improved dimensional tolerances for through-wafer fabrication approach vs the SOI fabrication approach.

Micro-Propulsion

MEMS-based Micro-Propulsion development has become an active area of research during the past decade for NASA and DoD agencies.[8-11] Controllable, ultra-low thrusts, down to the 0.1 micro-Newton range, with minimum controlled impulses as low as a few micro-Newton-seconds, are becoming a critical requirement for several, novel mission concepts currently being studied. For example, MEMS thrusters satisfying the above requirements could be needed for future interferometry missions such as Terrestrial Planet Finder (TPF), which require several spacecraft flying in precise formation, making up "long baseline" telescopes for detecting planets orbiting distant stars. Another application area is the stabilization of large inflatable spacecraft, offsetting the effects of solar pressure disturbances. The most demanding application, and perhaps the one for which MEMS thrusters are the only choice, is for providing primary propulsion and attitude control for micro-spacecraft. By definition, micro spacecraft have extremely limited resources and therefore have severe constraints on the size, mass and power consumption of components such as thrusters.

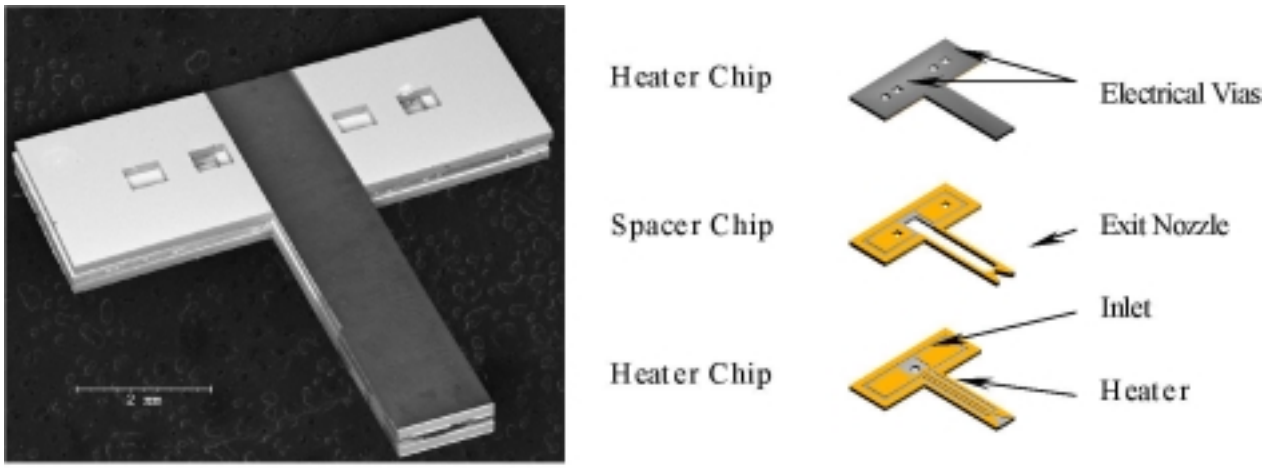

Figure 5. A Scanning Electron Micrograph of an assembled "T"-type Vaporizing Liquid Microthruster is shown on the left. The schematic exploded view shows the three-chip construction of the VLM. The liquid propellant is introduced through an inlet on the bottom chip, vaporized and exits via a nozzle defined by the middle, spacer chip.

The MEMS Technology Group has a strong involvement in an effort led by a sister JPL group, the Advanced Propulsion Technology Group. The effort is aimed at development of novel Micro-Propulsion devices for primary propulsion and attitude control of micro-spacecraft. These devices include among others, a Vaporizing Liquid Micro thruster[11] (described below) and a Field Emitter Array-based Electric Propulsion thruster. The collaborative effort hopes to fully exploit the unique, integration advantage of the MEMS approach, allowing a "quantum leap" in the reduction of the overall propulsion system size. Currently, propulsion systems are made up of discrete parts. Considerable savings in mass, size and external interfaces could be realized by fully integrated, miniature propulsion systems, combining the control electronics, microfluidics and the micro thruster functions in a single package.

The Vaporizing Liquid Micro-Thruster[11] (VLM) vaporizes a liquid propellant on demand to produce thrust. The primary application of the VLM is in attitude control of micro spacecraft, achieved by deploying several VLM modules around the spacecraft bus. The VLM consists of a bonded set of three, bulk-micromachined chips (Fig. 5), containing the inlet, heater element, flow channel and the nozzle through which the vaporized liquid exits to produce thrust. Water is being used as propellant in initial laboratory tests due to its safety and ease of use. A VLM of the type shown in Fig. 5 was recently tested on a thrust stand developed at JPL. This thrust stand is of a torsional spring design, and based on earlier versions developed at Princeton University[12]. Thrust data of 32 μN at power levels of 0.8 W were measured. The thrust was determined within an accuracy of about 0.5 μN. To date, no specific impulse data are available yet and data post processing continues. However, in previous tests mass flow rates through the thruster ranged around tenths of grams per hour under conditions in which the thruster successfully vaporized the injected flow rates completely without liquid droplet ejection.

Micro-valves

MEMS-based microfluidics[13] is an active area of research as evidenced by the number of research groups worldwide pursuing the development of microfluidic systems for numerous applications. Despite the large number of efforts, there is a critical lack of MEMS control valves with good performance characteristics. Part of this problem could be due to the drastic reduction of available actuation forces, which are typically directly proportional to the dimensions of the actuating member. The MEMS Technology Group is developing a novel piezoelectrically-actuated micro-valve[14] (Fig. 6) that is potentially capable of satisfying the rather stringent requirements for micro-propulsion applications. For pressurized cold gas thruster applications for instance, it is necessary for the micro-valve to be able to withstand a high inlet gas pressure (> 3000 psi), have a low leak rate (< 0.3 sccm), be capable of rapid actuation (1- 10 ms) and consume low power (<1 W). Initial test results of the JPL Micro Valve have been very encouraging. The valve was operated at frequencies of 10Hz –1kHz at low actuation voltages (~10V). In the closed condition, the valve had a leak rate below the detection threshold of 0.001 sccm at inlet pressures between 10 – 1000 psig.

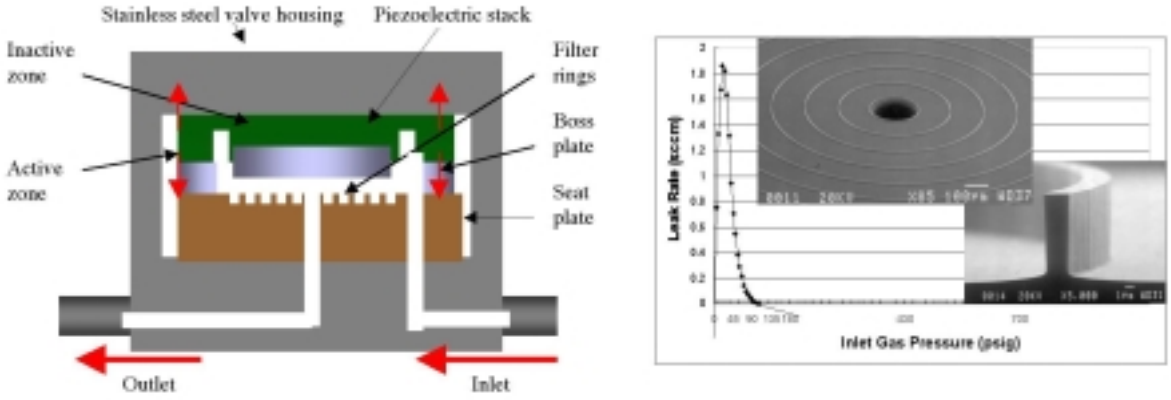

Figure 6. Cross-sectional schematic view of the Micro Valve is shown on the left. The actuation voltage is reduced considerably by the use of a "stacked" piezoelectric actuator. Shown on the right is the leak rate of the valve in the "passive" closed position versus applied inlet pressure. The design exploits the use of the inlet pressure to provide the sealing force and negligible leak rates are observed at inlet pressures above 100 psig. Two scanning electron micrographs are inset, showing a low magnification view of the inlet on the seat plate and a higher magnification view of a sealing ridge. The concentric sealing ridge design was developed as a mitigating measure in case of particulates being present in the flow.

Adaptive Optics

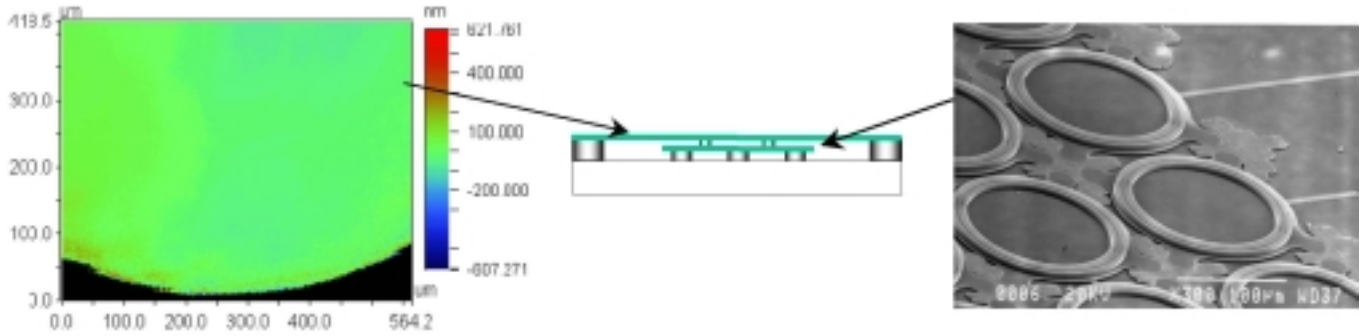

Figure 7. High stroke, continuous membrane, deformable mirror. The cross-sectional schematic in the center shows the two transferred membranes bonded via the thermocompression of In bumps. The scanning electron micrograph on the right shows a high magnification view of the corrugated actuator membrane. Surface profile measurement of the continuous, top membrane shows an optical quality surface

Several research groups[15-20] have developed micromachined versions of deformable mirrors to correct the blurring of images in telescopes caused by wavefront distortions accumulated during the atmospheric transmission of starlight. The segmented mirrors[15-17] approach in which individual pixels have tip/tilt capability is not suitable for astronomy applications because of edge diffraction effects resulting in an increased scattered light background. Continuous membrane approaches have been also been previously attempted[18-20] however, these have either suffered from inter-pixel actuator coupling effects[18,19] or did not possess the requisite mirror surface quality[20]. The MEMS Technology Group has developed a novel approach of using a 2-layer membrane transfer process to create a high-stroke, optical quality, micromachined deformable mirror[21,22] (Fig. 7). The process uses SOI wafers on which polysilicon layers have been deposited. The first layer to be transferred is the pixel actuation layer consisting of a corrugated polysilicon membrane patterned with the electrostatic actuation electrodes. Subsequently a continuous, optical quality, single crystal Si membrane is transferred onto the polysilicon actuator membrane. Inter-layer bonding is achieved via the thermo-compression of In bumps. Initial characterization results are very promising. A 1 μm thick polysilicon actuator membrane was successfully transferred onto a wafer substrate with previously fabricated deflection electrodes. The gap between the membrane and the electrode substrate is very uniform (+/- 0.1 μm across a wafer diameter of 100 mm, provided by optimizing the bonding control). A WYKO RST Plus optical profiler was used to measure the static deflection and the surface profile of transferred membranes. The fabricated polysilicon actuator with an electrode gap of 1.5 μm has a vertical deflection of 0.37 μm at 55 V. The surface profile of a transferred single crystal Si mirror membrane was measured is comparable to that of a typical silicon wafer. Thus, we have successfully obtained an optical quality deformable mirror using this process, by exploiting the fact that the transferred membrane is a replica of the carrier SOI wafer.

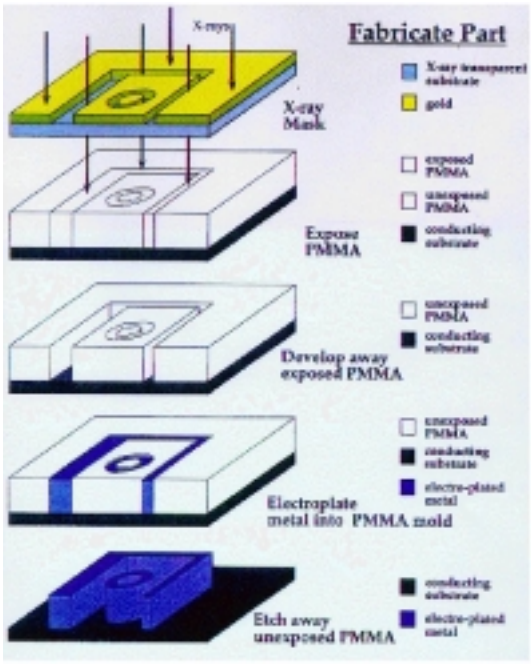

Figure 8. The LIGA process consists of first exposing a thick PMMA resist to collimated, synchrotron x-rays. The resist is subsequently developed and a MEMS structure is electroplated within the developed "mold".

LIGA activities

The MEMS Technology Group has invested heavily in the development of a "rapid turnaround" LIGA infrastructure in collaboration with Sandia National Laboratories (Livermore) and the Lawrence Berkeley Laboratory. The group has also established working relationships with the Stanford Linear Accelarator Center (SLAC) and Brookhaven National Laboratory. LIGA[23] is a German acronym for **LI**thographie **G**alvanoformung **A**bformung, which essentially describes the process of high aspect ratio lithography using collimated synchrotron x-rays followed by electroplating within the "micro-molds" created within the polymethylmethacrylate (PMMA) resist (see Fig. 8). The MEMS group is currently using the LIGA fabrication process to microfabricate the key components of a miniature Gas Chromatograph/Mass Spectrometer (GCMS) system. These components are the Quadrupole Mass Filter[24] (Fig. 9) and a miniature roughing pump based on the scroll pump approach. Additionally, the group is experimenting with 3-D LIGA fabrication techniques to produce axially symmetric structures that could be used as resonators for miniature gyroscopes. In the past the group has successfully demonstrated the proof-of-concept for high aspect ratio Au grids for X-ray Astronomy applications.

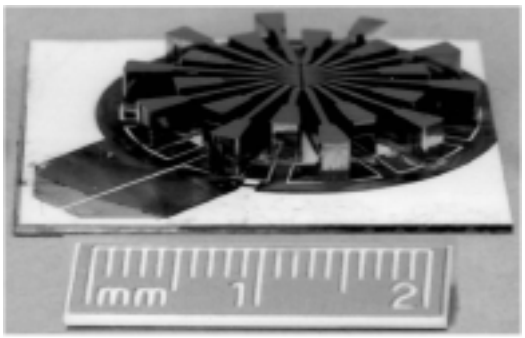

Figure 9. A prototype qudrupole mass filter component for a miniature GCMS system fabricated using the LIGA process

Tuned Band Emitter/Bolometer Gas Sensor

The development of the MEMS Tuned Band Emitter/Bolometer Gas Sensor[25-27] is an example of a successful collaboration between the MEMS Technology Group and a commercial firm, Ion Optics Inc. The objective of the development was to produce a low-cost, low power, gas detector based on the principle of infrared absorbing gas cell. Details of the gas sensor built around the core emitter/bolometer component are shown in Fig. 10. The device consists of a suspended filament of single crystal Si fabricated from an SOI substrate using a combination of surface micromachining and bulk micromachining techniques. The choice of single crystal Si was dictated by the exquisite sensitivity of the bolometric resistance to changes in temperature. At the operating temperature (few hundred degrees Celsius) the Si is essentially an intrinsic semiconductor with a negative, exponential dependence of resistance with temperature. The tuned emission property is achieved by lithographically patterning the filament surface (Fig. 10) with an array of hole-like features with a size and distribution such that the emissivity of the filament peaks at the gas absorption wavelength of interest. The highly reflective, metallized Si surface insures that the filament is a poor emitter outside the wavelength band of interest.

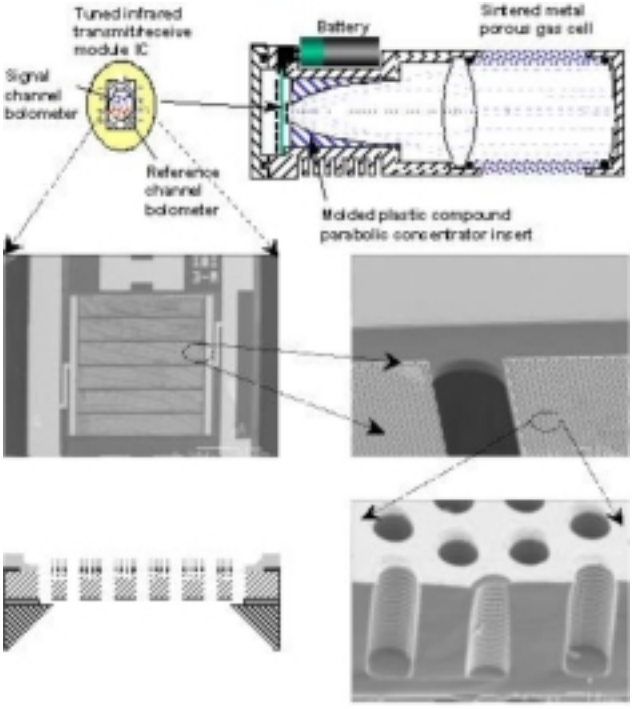

Figure 10. The MEMS Tuned Band Emitter/Bolometer Gas Sensor. As shown above, the gas sensor is constructed such that the infrared radiation is reflected back onto the emitter. The presence of the emission absorbing gas in the cell reduces the energy reflected back to the emitter, causing a temperature drop, which is measured as a change in the resistance of the emitter. The scanning electron micrographs are at progressively higher magnifications, showing the structure of the suspended, single crystal Si emitter/bolometer (shown in the cross-sectional schematic view).

The Tuned Emitter/Bolometer device has been fabricated, assembled and tested successfully in a vacuum chamber equipped with a valve for the introduction of CO_2. The device detected the presence of the introduced CO_2 at the fundamental infrared absorption peak of 4.3 μm. The focus of the current work is to reduce the sources of (primarily electrical) noise and to optimize the lithographic patterning on the filament surface to produce a narrow-band emission, minimizing variations in the azimuthal direction. Following device optimization, the next big challenge that will be tackled is to design and fabricate a compact package for the device.

Force Detected Nuclear Magnetic Resonance

Nuclear Magnetic Resonance (NMR) Spectroscopy is the premier spectroscopic method used for identification of chemical compounds. From a space exploration perspective, the power of NMR to be able to detect and identify the chemical state of water (whether physisorbed or chemisorbed) is very important. Few techniques are capable of such definitive identification. The primary focus of "astrobiological" investigations is to determine whether life exists or existed on other planets such as Mars. The origin and maintenance of life on earth requires the presence of water. Therefore, NMR spectroscopy, if it can be conducted using miniature instruments (the current versions are typically room-sized) could be a powerful tool for astrobiology missions. Conventional NMR is conducted using the "Faraday-law" detection technique, in which the excited nuclear spins induce a current in a search coil. The Force Detected NMR (FDNMR) technique[28] has better sensitivity than the conventional Faraday-law detection technique at the 0.5 mm length scale and below. This arises from the signal-to-noise ratio scaling as $d^{0.5}$ for the force detection technique, and as d^2 for conventional NMR (d: sample diameter). Other FDNMR approaches suffer from broadening of the NMR lines and losses in sensitivity due to the magnetic field gradient imposed on the sample. This problem is mitigated in the Caltech/JPL approach by producing a homogenous magnetic field across the sample using the symmetric magnet assembly[28] shown in Fig. 11. The FDNMR spectrometer consists of a harmonic oscillator made up of a detector magnet

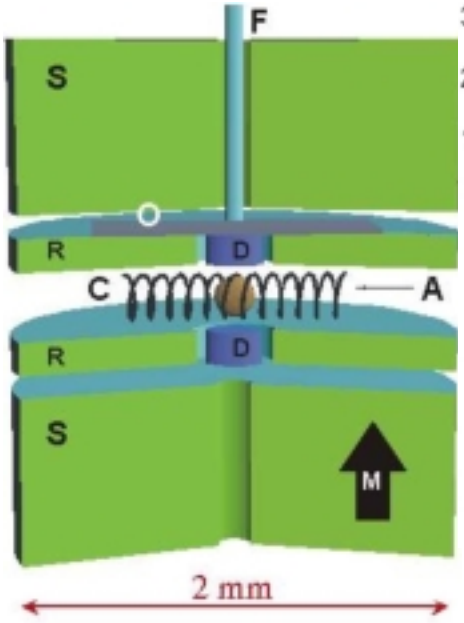

Figure 11. Cross-sectional schematic of the microfabricated FDNMR spectrometer. The field magnet (S) induces Zeeman splitting of nuclear spin levels in the sample. The detector magnet (D) mounted on the Si beam resonator (O) interacts with sample through dipole-dipole force, and the ring magnet (R) provides field uniformity across the sample. RF coil (C) modulates the dipole-dipole force at the mechanical resonance frequency of the oscillator. Fiber-optic interferometer (F) detects the motion of oscillator.

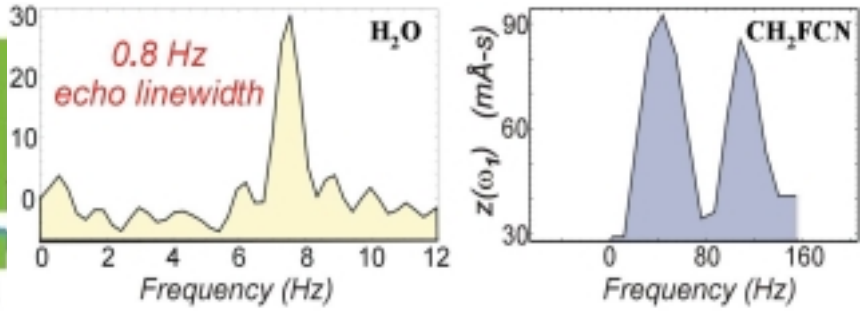

Figure 12. Proton FDNMR spectra of (a) H_2O and (b) CH_2FCN. The spectra were acquired with a prototype FDNMR which is 25 times the size of the final micro-fabricated device. (a) In the spectrum of H_2O, residual inhomogeneous broadening has been eliminated with spin-echo techniques and a line width of 0.8 Hz is achieved. (b) For CH_2FCN, an additional echo pulse sequence is applied to the F nuclei and H-F hetero nuclear decoupling is successfully observed.

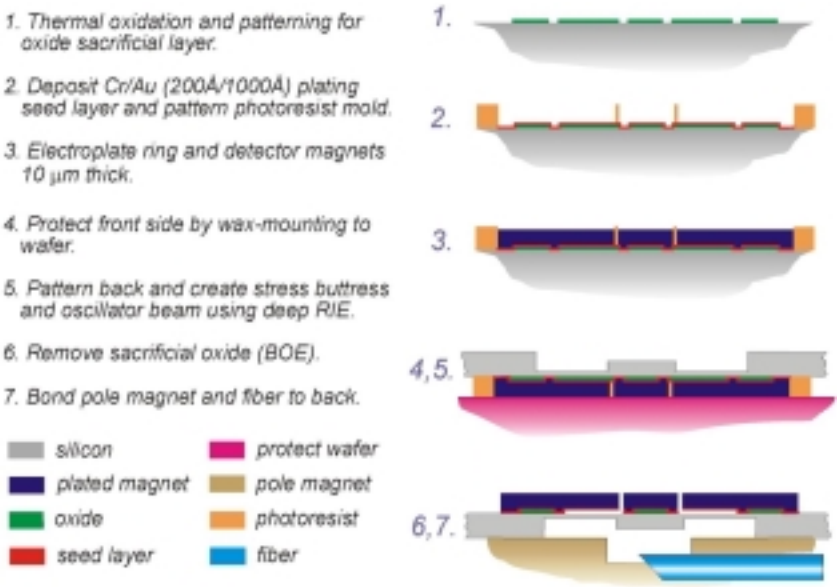

Figure 13. MEMS fabrication process for the FDNMR device shown in Fig. 11. The process is shown only for the top half of the device since the magnet assembly is symmetric.

mounted on a Si beam. The detector magnet sits within an annular magnet and thus provides a uniform magnetic field over the entire sample volume. Rf pulses applied to the sample modulate the dipole-dipole interaction between the nuclear magnetic moment of the sample and the detector magnet at the mechanical resonance frequency of the resonator. The resulting motion of the mechanical resonator is detected using a fiber-optic interferometer with background noise nearly at the Brownian-motion limit. Figure 12 shows proton NMR spectra of H_2O and CH_2FCN obtained with our mm-scale prototype FDNMR device. These spectra show the chemical specificity and applicability of our FDNMR method, and the experimental data agrees quantitatively with theoretical sensitivity predictions.

Figure 13 shows the processing sequence for the microfabricated FDNMR device. Detector and ring magnets are first electrodeposited. High aspect ratio (10:1) photoresist (PR) separates the detector magnet from the ring magnet and creates radial slits in the ring magnet during electro-deposition. The radial slits serve to reduce eddy current damping and we have observed a "Q" increase of a factor of 3 with 32 slits in the ring magnet of our prototype. Various magnetic

materials have been electrodeposited to achieve high magnetic saturation field with low stress and high corrosion resistance. Electrodeposited CoNiFe (Ni:5-13% and Fe:5-50%) films have promising magnetic properties (Ms up to 2.1 T) with good corrosion resistance. The electrodeposition step is followed by the microfabrication of a resonator beam using DRIE. A three-step DRIE fabrication process is used to produce the beam and has advantages over using a conventional SOI wafer process, in achieving efficient fabrication, as well as in the post-testing adjustment of the beam thickness and thereby its resonance frequency. The measured mechanical resonant frequencies of our 2-6 mm thick beams are 24-166 kHZ, which are appropriate for FDNMR measurements and agree with theoretical predictions to within 5%. The Q's measured for these beams have values of 500 at 1 atm and 5000 at 50 mtorr.

Nano-mechanical Resonator Development

Nano Electro Mechanical Systems (NEMS) has become in vogue with the recent worldwide emphasis on Nanotechnology[29]. The approach adopted by the MEMS Technology Group is to use the state-of-the-art, 8-nm-resolution, electron beam lithography system available at the MDL to fabricate NEMS structures, specifically nano-mechanical resonators for spectroscopy and high frequency (300 MHz – 3 GHz) rf communication applications. The Caltech/JPL-proposed "Force-Detected Optical Spectroscopy", as shown is Fig. 14, is aimed at the detection of single molecules via an electric dipole-dipole interaction, that is modulated optically at the mechanical resonance frequency of the nano-mechanical resonator (~ 500 MHz). Electron Beam Lithography-based NEMS fabrication was used 40-nm-sized arrays of Au dots and 1 μm x 100 nm x 100 nm Si beams for the FDOS and rf communication applications.

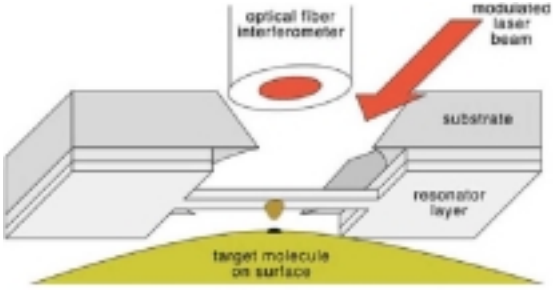

Figure 14. Schematic of the Force Detected Optical Spectrometer. An electric dipole-dipole interaction between the target molecule and a bulk plasmon in a nano Au dot is modulated by an external laser beam at the resonance frequency of nano-mechanical Si resonator beam. The motion of the Si nano-beam fabricated from an SOI wafer is detected interferometrically.

"PICOSAT" Space Test Program

A major problem that is endemic to low TRL MEMS/NEMS development is that it is extremely hard for these technologies to make the transition to flight sytems/sub-systems. As mentioned above the TRL "gap" represents both the extensive development time and corresponding expense involved in producing reliable systems capable of withstanding the rigors of the launch, flight and deployment environments. To a large extent this could also be considered a "perception" problem, since mission planners are understandably risk averse. They want very much to avoid dependence on technologies without space "heritage", that could potentially cause a failure of these high visibility, highly expensive, planetary missions. Also, as mentioned above NASA's NMP has limited flight opportunities to space test new technologies. Thus, a low-cost, rapid launch, space testing program is badly needed to ensure a high return on the extensive investment made by NASA and other agencies into MEMS/NEMS technologies.

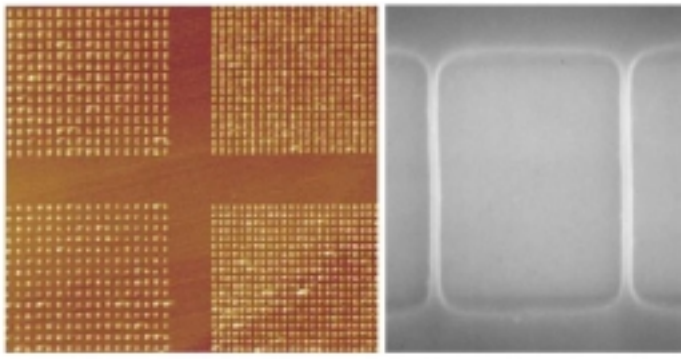

Figure 15. Electron Beam Lithography was used to fabricate arrays of 40-nm-sized Au dots (left) and Si beams (1 μm x 100 nm x 100 nm) for the FDOS application.

DARPA/AFRL have initiated a very exciting, low cost, rapid space testing program via the use of "PICOSAT" space platforms, originally invented by the Aerospace Corporation[30]. These PICOSATs are specifically meant to be MEMS/NEMS space test platforms, culminating in the development of a MEMS-based PICOSAT Inspector (MEPSI) spacecraft. The design principle used to make these missions extremely low cost and to also have rapid launch capability is to build a standardized, low mass (<1 kg) spacecraft bus that can take advantage of practically any launch opportunity in a "minimally invasive" manner. Once released in low earth orbit, the PICOSAT is completely

independent and does not require any resources from the primary spacecraft. Two such PICOSAT missions, have already been successfully demonstrated in space (Fig. 16). Starting in 2001, under DARPA/AFRL funding, the MEMS Technology Group is partnering with the Aerospace Corporation on a joint project to space test a broad range of MEMS devices for inertial guidance, primary propulsion and attitude control, and rf communication. The MEPSI project has been assigned 6 space test flights over the next few years by the Space Test Program of the Department of Defense. The MEPSI team is working towards establishing collaborations with universities and other research centers interested in rapid space testing experiments. It is our hope, that once established, this exciting program can be expanded to support the space test needs for a wide range of MEMS/NEMS technologies being developed at JPL and other institutions. The PICOSAT platform also has the potential to test, at a fraction of the cost, a wide range of mission architectures that are being contemplated for the future.

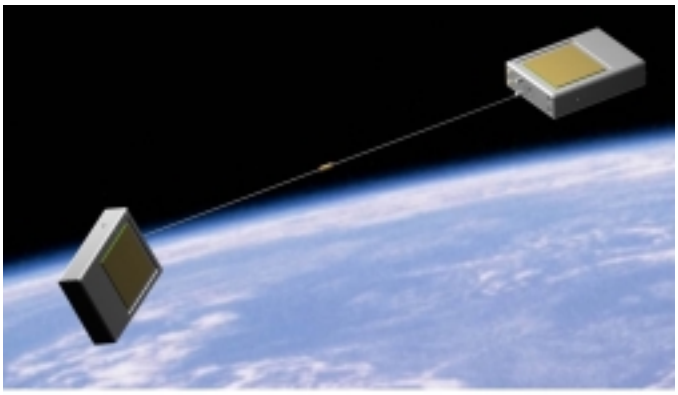

Figure 16. Artist's conception of a pair of deployed PICOSATs in low earth orbit. Each PICOSAT is a 25mm x 75mm x 100mm aluminum box containing a lithium thionyl chloride primary battery, stack of electronics boards for the flight computer, rf communication, MEMS testing and power management. Each PICOSAT contained a 64 mW, 915 MHz radio for communication with earth and between each other. The MEMS payload on each PICOSAT was an RF MEMS switch. The PICOSATs were tethered together with a 33 m, metallized line to keep them within communication distance of each other and to be easily detectable by ground-based tracking radar.

ACKNOWLEDGEMENTS

The MEMS/NEMS technology developments reported in this paper were carried out by members of the MEMS Technology Group in collaboration with personnel from other research groups at JPL, universities, commercial companies and other research facilities. The work described in this paper was supported primarily by NASA's Cross Enterprise Technology Development Program, the Center for Integrated Space Microsystems, the Herschel/Planck Flight Missions, the Air Force Research Laboratory and the Defense Advanced Research Projects Agency (DARPA). Other sponsors include commercial sponsors and the JPL Director's Research and Development Fund.

REFERENCES

1. For more information on currently planned and future NASA missions, please refer to the NASA website: http://www.nasa.gov
2. For information on NASA's New Millennium Program please refer to URL: http://nmp.jpl.nasa.gov/
3. A. D. Turner, J. J. Bock, J. W. Beeman, J. Glenn, P. C. Hargrave, V. V. Hristov, H. T. Nguyen, F. Rahman, S. Sethuraman, and A. L. Woodcraft, "Silicon Nitride Micromesh Bolometer Array for Submillimeter Astrophysics", *Applied Optics* 40, 4921 (2001).
4. A.H. Jaffe, P.A.R. Ade, A. Balbi, J.J Bock, J.R. Bond, J. Borrill, A. Boscaleri, K. Coble, B.P. Crill, P. de Bernardis, P. Farese, P.G. Ferreira, K. Ganga, M. Giacometti, S. Hanany, E. Hivon, V.V. Hristov, A. Iacoangeli, A.E. Lange, A.T. Lee, L. Martinis, S. Masi, P.D. Mauskopf, A. Melchiorri, T. Montroy, C.B. Netterfield, S. Oh, E. Pascale, F. Piacentini, D. Pogosyan, S. Prunet, B. Rabii, S. Rao, P.L. Richards, G. Romeo, J.E. Ruhl, F. Scaramuzzi, D. Sforna, G.F. Smoot, R. Stompor, C.D. Winant, J.H.P. Wu, "Cosmology from Maxima-1, Boomerang and COBE/DMR CMB Observations", *Physical Review Letters* 86, 3475-3479 (2001).
5. T. Tang, W. Kaiser, R. Bartman, R. Gutierrez, J. Wilcox, R. Calvet and S.K. Tsang, "Silicon Bulk Micromachined, Symmetric, Degenerate Vibratory Gyroscope, Accelerometer and Sensor and Method for Using the Same", *US Patent* No. 5,894,090, issued April 1999.
6. S. Y. Bae, D. V. Wiberg, K. J. Hayworth and K.Y. Yee, "High Performance MEMS Micro-Gyroscope", *This Symposium proceedings,* 2002.
7. K. Shcheglov, "Fabrication Process for Meso Scale Micromachined Gyroscope", *NASA New Technology Report*, NPO–30288.

8. J. Mueller, E.H. Yang, A. Green, V. White, I. Chakraborty, and R. Reinicke, “Design and Fabrication of MEMS-Based Micropropulsion Devices at JPL”, *SPIE Micromachining Conference Proceedings*, San Francisco, 2001.
9. J. Mueller, C. Marrese, J. Polk, E.H. Yang, A. Green, V. White, D. Bame, I. Chakraborty, and S. Vargo, "An Overview of MEMS-Based Micropropulsion Developments at JPL", Paper IAA-B3-1004, Presented at the 3rd International Symposium of the International Academy of Astronautics (IAA) for Small Satellites for Earth Observation, Berlin, Germany, April 2-6, 2001, to be published in *Acta Astronautica*, December 2001
10. J. Mueller, “Thruster Options for Microspacecraft: A Review and Evaluation of State-of-the-Art and Emerging Technologies”, *Micropropulsion for Small Spacecraft, Progress in Astronautics and Aeronautics*, Vol. 187, edited by Micci, M. and Ketsdever, A., AIAA , Reston, VA, 2000, Chap. 3.
11. J. Mueller, I. Chakraborty, D. Bame, and W. Tang, “The Vaporizing Liquid Micro-Thruster Concept: Preliminary Results of Initial Feasibility Studies”, *Micropropulsion for Small Spacecraft, Progress in Astronautics and Aeronautics*, Vol. 187, edited by Micci, M. and Ketsdever, A., AIAA , Reston, VA, 2000, Chap. 8.
12. Cubbin, E.A., Ziemer, J.K., Choueiri, E.Y., and Jahn, R.G., "Pulsed Thrust Measurements using Laser Interferometry", *Rev. Sci. Instrum*., 68 (6), pp. 2339 - 2346, June 1997.
13. A.D. Stroock, S.K.W. Dertinger, A. Ajdari, I. Mezic, H.A. Stone and G.M. Whitesides, “Chaotic Mixer for Microchannels”, *Science* 295, 647 (2002).
14. E.H. Yang, N. Rohatgi and L. Wild*, “*Design, Fabrication and Test of a MEMS-based Valve for Micropropulsion Applications”, *NASA New Technology Report*, NPO- 30158.
15. V.M. Bright *et al*., ”Surface micromachined micro-opto-electro-mechanical systems,” *IEICE Trans. Electron*., vol. E80-C., No. 2, 206-213 (1997).
16. M.A. Michalicek *et al*., “Design and simulation of advanced surface micromachined micro mirror devices for telescope adaptive optics applications,” *Proc. SPIE Conf. on Adaptive Optical System Technology*, Kona, Hawaii, 805-815 (1998).
17. W.D. Cowan *et al*., “Evaluation of microfabricated deformable mirror systems,” *Proc. SPIE Conf. on Adaptive Optical System Technology*, Kona, Hawaii, 790-804 (1998).
18. G. Vdovin, “Optimization-based operation of micromachined deformable mirrors,” *Proc. SPIE Conf. on Adaptive Optical System Technology*, Kona, Hawaii, 902-909 (1998).
19. P.K.C. Wang *et al*., “A method for designing electrostatic-actuator electrode pattern in micromachined deformable mirrors,” *Sensors and Actuators A*, Vol. 55, 211-217 (1996).
20. T. Bifano *et al*., “Continuous-membrane surface-micromachined silicon deformable mirror,” *Opt. Eng.*, 36(5) 1354 (1997).
21. E.H. Yang and D.V. Wiberg, "A Wafer Transfer Technology for MEMS Adaptive Optics," *Proceedings of the ASME International Mechanical Engineering Congress and Exposition*, Novel Micromachining Processes and Packaging for MEMS, New York, New York, November 2001.
22. E.H. Yang and D.V. Wiberg, "A New Wafer-Level Membrane Transfer Technique for MEMS Deformable Mirrors," *Proceedings of the IEEE International Conference on Microelectromechanical Systems (MEMS i01) Conference*, Interlaken, Switzerland, Jan. 2000, pp. 80-83.
23. H. Guckel, “High-aspect-ratio micromachining via deep x-ray lithography”, *Proc. IEEE*, 86, 1586 (1998).
24. D. Wiberg, M. Hecht, O. Orient, A. Chutjian, K. Yee, S. Fuerstenau, R. Brennen, W. Bonivert, J. Hruby, and K. Jackson, "A LIGA Fabricated Quadrupole Array for Mass Spectroscopy", *HARMST '97*, Madison, WI, 20-21 (1997).
25. T. George, E.W. Jones and D. Choi, “ Micromachined Tuned Band Hot Bolometer Emitter”, US Patent application submitted.
26. J.T. Daly, A.C. Greenwald, E.A. Johnson, W.A. Stevenson, J.A. Wollam, T. George, and E.W. Jones, “Nano-Structured Surfaces For Tuned Infrared Emission For Spectroscopic Applications”, *SPIE* 3937-14, (2000).
27. H. Jones-Bey, “MOEMS bolometer may provide cost-effective optical gas sensing”, *Laser Focus World*, Article No. 130129, December 2001.
28. G. M. Leskowitz, L. A. Madsen, D. P. Weitekamp, *Sol. St. Nucl. Magn. Reson.* 11, 73 (1998).
29. See: “Nanostructure Science and Technology: A Worldwide Study”, a World Technology Evaluation Center (WTEC) study report, at URL: http://www.wtec.org/loyola/nano/
30. S. W. Janson, H. Helvajian and E.Y. Robinson, “The Concept of ‘Nanosatellite’ for Revolutionary Low-Cost Space System”, Paper No. IAF-93-U.5.573, 44th IAF Congress, Graz, Austria (1993).